CORA Cork Open Research Archive
Cartlann Taighde Oscailte Chorcaí

Title	Monolayer doping of silicon-germanium alloys: a balancing act between phosphorus incorporation and strain relaxation
Authors	Kennedy, Noel;Duffy, Ray;Mirabelli, Gioele;Eaton, Luke;Petkov, Nikolay;Holmes, Justin D.;Hatem, Chris;Walsh, Lee;Long, Brenda
Publication date	2019-07-09
Original Citation	Kennedy, N., Duffy, R., Mirabelli, G., Eaton, L., Petkov, N., Holmes, J. D., Hatem, C., Walsh, L. and Long, B. (2019) 'Monolayer doping of silicon-germanium alloys: A balancing act between phosphorus incorporation and strain relaxation', Journal of Applied Physics, 126 (2), 025103 (9 pp). 10.1063/1.5086356
Type of publication	Article (peer-reviewed)
Link to publisher's version	https://aip.scitation.org/doi/abs/10.1063/1.5086356 - 10.1063/1.5086356
Rights	© 2019, AIP Publishing. This article may be downloaded for personal use only. Any other use requires prior permission of the author and AIP Publishing. The following article appeared in Journal of Applied Physics 126:2 and may be found at https://aip.scitation.org/doi/abs/10.1063/1.5086356
Download date	2026-11-01 13:19:34
Item downloaded from	https://hdl.handle.net/10468/8389

UCC
University College Cork, Ireland
Coláiste na hOllscoile Corcaigh

Journal of Applied Physics

Monolayer doping of silicon-germanium alloys: A balancing act between phosphorus incorporation and strain relaxation

Cite as: J. Appl. Phys. **126**, 025103 (2019); https://doi.org/10.1063/1.5086356
Submitted: 20 December 2018 . Accepted: 16 June 2019 . Published Online: 09 July 2019

Noel Kennedy, Ray Duffy, Gioele Mirabelli, Luke Eaton, Nikolay Petkov, Justin D. Holmes, Chris Hatem, Lee Walsh, and Brenda Long

View Online Export Citation CrossMark

ARTICLES YOU MAY BE INTERESTED IN

Spectral broadening in self-assembled GaAs quantum dots with narrow size distribution
Journal of Applied Physics **126**, 024301 (2019); https://doi.org/10.1063/1.5097277

Lattice dynamics and lattice thermal conductivity of $CrSi_2$ calculated from first principles and the phonon Boltzmann transport equation
Journal of Applied Physics **126**, 025105 (2019); https://doi.org/10.1063/1.5096458

Double Gaussian distribution of barrier heights and self-powered infrared photoresponse of InN/AlN/Si (111) heterostructure
Journal of Applied Physics **126**, 025301 (2019); https://doi.org/10.1063/1.5100066



AIP Publishing

© 2019 Author(s).

Journal of Applied Physics ARTICLE scitation.org/journal/jap

Monolayer doping of silicon-germanium alloys: A balancing act between phosphorus incorporation and strain relaxation

Cite as: J. Appl. Phys. **126**, 025103 (2019); doi: 10.1063/1.5086356
Submitted: 20 December 2018 · Accepted: 16 June 2019 ·
Published Online: 9 July 2019

View Online Export Citation CrossMark

Noel Kennedy,[1,2,3] Ray Duffy,[2,a)] Gioele Mirabelli,[2] Luke Eaton,[1,2,3] Nikolay Petkov,[4] Justin D. Holmes,[1,2,3] Chris Hatem,[5] Lee Walsh,[2] and Brenda Long[1,2,3,a)]

AFFILIATIONS

[1]School of Chemistry, University College Cork, Cork T12 YF78, Ireland
[2]Tyndall National Institute, Lee Maltings, Cork T12 R5CP, Ireland
[3]CRANN@AMBER, Trinity College Dublin, Dublin 2, D02 E16, Ireland
[4]Cork Institute of Technology, Bishopstown, Cork T12 T66T, Ireland
[5]Applied Materials, Gloucester, Massachusetts 01930, USA

[a)]**Authors to whom correspondence should be addressed:** brenda.long@ucc.ie and ray.duffy@tyndall.ie

ABSTRACT

This paper presents the application of monolayer doping (MLD) to silicon-germanium (SiGe). This study was carried out for phosphorus dopants on wafers of epitaxially grown thin films of strained SiGe on silicon with varying concentrations of Ge (18%, 30%, and 60%). The challenge presented here is achieving dopant incorporation while minimizing strain relaxation. The impact of high temperature annealing on the formation of defects due to strain relaxation of these layers was qualitatively monitored by cross-sectional transmission electron microscopy and atomic force microscopy prior to choosing an anneal temperature for the MLD drive-in. Though the bulk SiGe wafers provided are stated to have 18%, 30%, and 60% Ge in the epitaxial SiGe layers, it does not necessarily mean that the surface stoichiometry is the same, and this may impact the reaction conditions. X-ray photoelectron spectroscopy (XPS) and angle-resolved XPS were carried out to compare the bulk and surface stoichiometry of SiGe to allow tailoring of the reaction conditions for chemical functionalization. Finally, dopant profiling was carried out by secondary ion mass spectrometry to determine the impurity concentrations achieved by MLD. It is evident from the results that phosphorus incorporation decreases for increasing mole fraction of Ge, when the rapid thermal annealing temperature is a fixed amount below the melting temperature of each alloy.

Published under license by AIP Publishing. https://doi.org/10.1063/1.5086356

INTRODUCTION

Device sizes for electronic applications have been aggressively scaled down over the past 50 years, pushing the limits of what was capable by introducing new materials such as high-k dielectrics[1] and new device architectures such as FinFETs,[2] for example. Regardless, in recent times, device dimensions have approached a critical point where silicon, the cornerstone of the semiconductor industry, struggles to achieve the performance gains as scaling continues. In this context, other high mobility materials, such as SiGe, are being investigated to assess their potential.[3] Currently, low mole fraction (MF) SiGe is being used as a stress enhanced carrier mobility booster[4] and is considered to be a viable candidate for a channel material in MOSFETs.[5–7] Recently, the 7-nm technology node solution has also been proposed with the integration of SiGe p-MOSFETs and strained-Si n-MOSFETs, showing the feasibility of SiGe devices in the future.[8] However, there are no reports of chemical functionalization of SiGe in the literature and only a few reports of *ex situ* doping SiGe[9,10] when compared to silicon.

For thin-film homogeneous strained or relaxed SiGe with >50% Ge content, there is little available experimental data on processing such as dopant diffusion and activation, contact formation, or on *in situ* doping and selective epitaxial growth on surfaces with different crystal orientations. Very recently, publications have emerged on high-Ge content SiGe for solar cell applications.[11–13]

Published under license by AIP Publishing.

Doping of future technology devices fabricated either from thin films or 3-dimensional structures could prove difficult for ion implantation, which has been the most commonly used *ex situ* doping technique during the device miniaturization drive until this point.[14,15] High energy ion beams induce damage (amorphization) into these structures that prove difficult to remove, if at all.[16] Possibly, the most critical flaw of ion implantation is the lack of conformality seen when doping 3-dimensional structures such as fins or nanowires. Due to the directionality of the technique, it struggles to equally dope both the top and sidewalls of these structures.[17] A number of alternative *ex situ* doping methods have been proposed and developed to offer solutions to the problems encountered with ion implantation such as plasma doping (PLAD),[18] spin-on-doping,[19] and solid-source-diffusion.[20] However, these techniques also suffer from crystal damage or lack of dose control. Doping SiGe *in situ* has been studied for many years[21–23] and is the current trend in certain technology applications. Furthermore, a boost in dopant activation by using a laser anneal after the growth of the *in situ* doped epi-layer has shown to be beneficial in source/drain contact regions.[24] However, for alternative applications or other parts of the transistor, epitaxy may not be suitable due to design or space restrictions.

Monolayer doping (MLD) has been developed as a method to produce ultrashallow junctions (USJ's) without crystal damage, while also conformally doping 3-dimensional substrates.[25–27] It has already been demonstrated on a variety of semiconductors, including Si,[28–34] Ge,[35–37] and a number of III-V materials.[38] Figure 1 depicts the MLD procedure on SiGe. The key step involves functionalization of the target surface through the bonding of a dopant molecule [in this case allyldiphenylphosphine (ADP)] to form a self-limiting monolayer where the quantity of dopant molecules present is determined by the molecule size and also defines the dose. Once monolayer formation is complete, the samples are capped with an oxide layer to prevent desorption and promote diffusion of the dopant atoms into the substrate during thermal treatments. After thermally treating the samples, the capping layer can be removed to leave a uniformly doped substrate whether it be planar or 3-dimensional. This paper will examine the application of phosphorous MLD to SiGe alloys ranging from a low Ge content

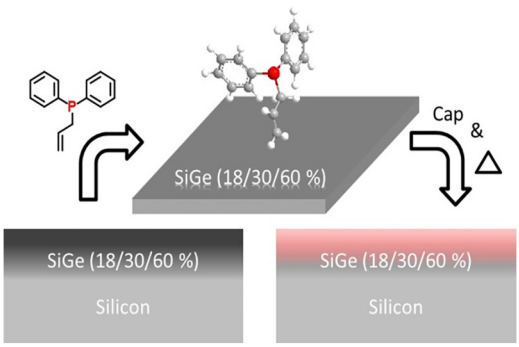


FIG. 1. Summary of MLD procedure on SiGe.

18% to a high Ge content 60% aiming to understand if this novel doping technique can effectively dope these substrates. There are two main challenges associated with doping SiGe by MLD: (1) how to chemically functionalize the SiGe with dopant-containing molecules (i.e., will the reactivity of the surface atoms to the molecules be like silicon or germanium?) and (2) how to avoid strain relaxation of the nonbuffered SiGe layers during the dopant drive-in annealing step?

EXPERIMENTAL

Thin films of strained SiGe were grown on a 300 mm Applied Materials epitaxy system on silicon substrates with germanium content of 18%, 30%, and 60%, respectively. The thickness of these films was inspected with cross-sectional transmission electron microscopy (XTEM). All chemicals were purchased from Sigma-Aldrich. $1 \times 1\ cm^2$ samples were cut from the starting SiGe wafers and cleaned by sonicating in acetone (≥99.8%) for 2 min, followed by rinsing in isopropyl alcohol (IPA-99.9%) and drying under a stream of nitrogen. Samples were hydrogen terminated by dipping in 2% hydrofluoric acid (HF) for 10 s and placed under nitrogen in a Schlenk line to prevent reoxidation. A 0.1M solution of allyldiphenylphosphine (ADP-95%) in mesitylene (98%) was degassed and transferred into the reaction flask containing the H-terminated samples. This reaction flask was heated to 180 °C for 3 h to allow for optimal monolayer formation on the SiGe surface. Samples were then removed and sonicated in IPA for 1 min followed by a further IPA rinse and drying under a stream of nitrogen to remove any physisorbed dopant molecule. Functionalized samples were stored under nitrogen until capping with 50 nm sputtered SiO_2. Rapid thermal annealing (RTA) was carried out at a variety of temperatures and times which are specified for each result. The SiO_2 capping layer was then removed by dipping in a 25:1 BOE solution until a hydrophobic H-terminated surface was produced.

Secondary ion mass spectrometry (SIMS) data were acquired on a Phi Adept 1010 using a 0.5–1 keV Cs+ bombardment with negative ion detection. Calibration was carried out using SiGe that has been implanted with P and measured using RBS (Rutherford backscattering spectrometry) to determine composition. Atomic force microscopy (AFM) was implemented in tapping/noncontact mode at room temperature over a $3 \times 3\ \mu m^2$ scanning area. A Kratos ULTRA spectrometer was used for X-ray photoelectron spectroscopy (XPS) measurements with the following parameters. Sample temperature was kept between 20 and 30 °C with a monochromated Al K α source used. Pass energies of 160 eV for survey spectra and 20 eV for narrow regions were used with steps of 1 eV (survey) and 0.05 eV (narrow regions). Dwell times were 50 ms (survey) and 100 ms (regions) while 12 sweeps were carried out during survey spectra, and for narrow region analysis from 5 to 40 sweeps were used. For structural analysis, FEI's Dual Beam Helios Nanolab 600i system using a Ga ion beam was used to obtain cross-sectional samples. Electron beam C, electron beam Pt, and ion beam C were used as protective layers. Lamellas were thinned and polished at 30 kV 100 pA and 5 kV 47 pA, respectively. JEOL 2100 HRTEM operated at 200 kV in the Bright Field mode using a Gatan Double Tilt holder was used for XTEM imaging.

Published under license by AIP Publishing.

RESULTS AND DISCUSSION

Figure 1 broadly describes the process of doping SiGe by MLD. ADP was chosen as a source of phosphorus for these experiments for two reasons: (1) it contains the C═C functionality that reacts with both Ge and Si, an assumption being made that it will also react with SiGe and (2) its remaining functional groups are phenyl rings that are highly unreactive thereby inhibiting multilayer formation. Epitaxially grown SiGe with varying concentrations of Ge were used in this study. As received, the amount of Ge in the SiGe wafers provided was stated to be 18%, 30%, and 60%. Representative XTEM images are shown in Fig. 2. Though chemical reactions on Si and Ge are similar, there are variations in reactivity between the two materials. For example, the reaction of an alkene with hydrogen terminated Si will occur in the solution when heated to 180 °C, but under these same conditions, it will not react with Ge. Either much higher temperature (>220 °C) or UV light is required for the reaction between an alkene and Ge to proceed.[35,36]

Though the bulk SiGe wafers provided are stated to have 18%, 30%, and 60% Ge in the epitaxial SiGe layers, it does not necessarily mean that the surface stoichiometry is the same as the bulk. The surface stoichiometry is important as it may impact the chosen reaction conditions for the chemical functionalization. In order to assess if surface stoichiometries differ to the bulk, an angle-resolved XPS study was carried out. Table I shows the measured stoichiometries for each sample.

The measured stoichiometries are 14%, 33%, and 65% for XPS with a takeoff angle of 90°, which corresponds to a sampling depth of 9.1 nm for the Ge 3d peak and 8.8 nm for Si 2p peak.[39] Those measured for the XPS with a takeoff angle of 60° were 12%, 31%, and 65%, where the sampling depth is halved when compared with samples measured with a takeoff angle of 90° and thus are more surface sensitive. With a commonly specified error range of ±10%, it can be concluded that the surface and bulk stoichiometries do not differ drastically.

Figure 3 shows roughly how much space the ADP will take up on the surface of a substrate. For the purposes of illustration, the surface depicted is silicon. Given that ADP has an approximate molecular footprint of 1 nm^2 and that the Si—Si bond length in crystalline Si is roughly 0.25 nm, about 1 in 16 Si atoms (or ~6% of the surface atoms) will have a molecule bonded to them. An assumption is made here that these calculations will be very similar for the SiGe substrates. Though these calculations and the illustration in Fig. 3 are for indication only, when combined with the XPS data, we are satisfied that we can treat the SiGe surface, from a chemical reactivity point of view, as if it were silicon. It should be noted that the authors recognize that though the chemical reactivity of Si and Ge are well established,[28,29,36,37] there is no available data on the reactivity of SiGe.

The selection of the drive-in anneal temperature is a critical part of this experimental setup. Si melts at 1416 °C, while Ge melts at 938 °C, and alloys of SiGe melt at temperatures between those extremes, depending on the % Ge content. Another consideration is that the epitaxial SiGe is strained, and heating to high temperatures will cause strain relaxation. XTEM and AFM were carried out on SiGe 30% to assess the impact of annealing at high temperature. The standard annealing temperature for MLD on Si is 1050 °C.[26,32] Before anneal, the substrates show no obvious crystal defects in the cross section or in the AFM analysis [representative images in Fig. 4(a)]. Postanneal at 1050 °C, it is obvious the SiGe layer has been degraded [Fig. 4(b)]. For example, there is extensive crosshatching in the AFM. Crosshatching occurs as a result of misfit dislocations having formed at the SiGe:Si interface. These misfit dislocations are an indication of the strain relaxation that can also

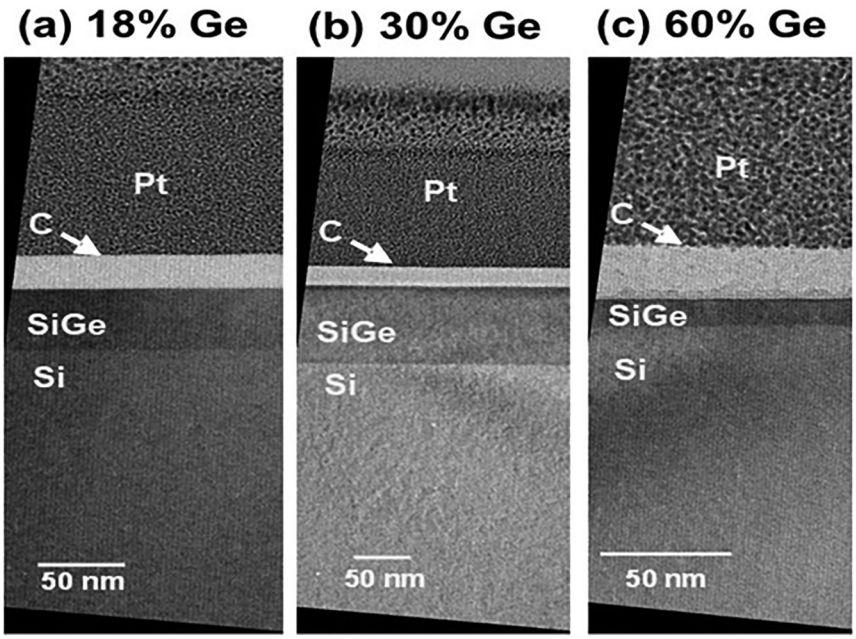


FIG. 2. XTEM of the as-received SiGe: (a) 18% Ge, (b) 30% Ge, and (c) 60% Ge.

Published under license by AIP Publishing.

TABLE I. The experimentally measured surface stoichiometries of the epitaxial SiGe. The measured stoichiometries are reported for takeoff angles of 90° and 60°. The measured stoichiometries are calculated from the areas of the Si *2p* and Ge *3d* XPS core levels, normalized using the appropriate relative sensitivity factors.

Sample ID	Measured stoichiometry	Measured stoichiometry (60°)
SiGe18	$Si_{0.86}Ge_{0.14}$	$Si_{0.88}Ge_{0.12}$
SiGe30	$Si_{0.67}Ge_{0.33}$	$Si_{0.69}Ge_{0.31}$
SiGe60	$Si_{0.35}Ge_{0.65}$	$Si_{0.35}Ge_{0.65}$

be seen in the XTEM that contains a noticeably defective SiGe:Si interface. Furthermore, a stacking fault is visible in Fig. 4(b) resulting in a kink or steplike feature at the surface where it terminates.

Due to this degradation, it is assumed that a 1050 °C RTA used for Si cannot be applied to Ge, and thus we are unable to apply a constant RTA temperature across all the SiGe alloys studied here. Instead, we have chosen an RTA temperature at a fixed amount below the melting temperature of each material, in accordance with Fig. 5. As 1050 °C is routinely used for P in-diffusion into Si,[34] we used this as our basis for a constant $T_{melt} - T_{RTA}$ (1416–1050 °C) value. The RTA temperatures for 18%, 30%, and 60% Ge content SiGe are thus 935, 835, and 685 °C, respectively.

Figure 6 shows AFM images of all SiGe samples before and after MLD processing. Samples before MLD show that the surface

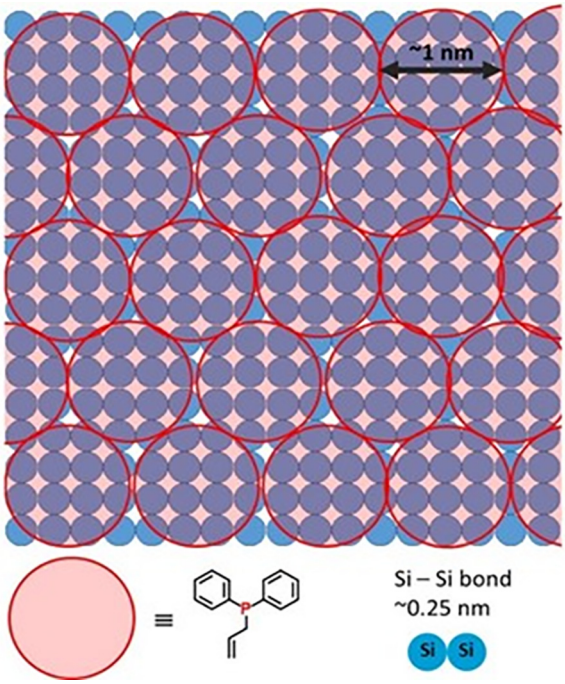


FIG. 3. Illustration showing the approximate footprint of the molecule, ADP, on the surface of silicon.

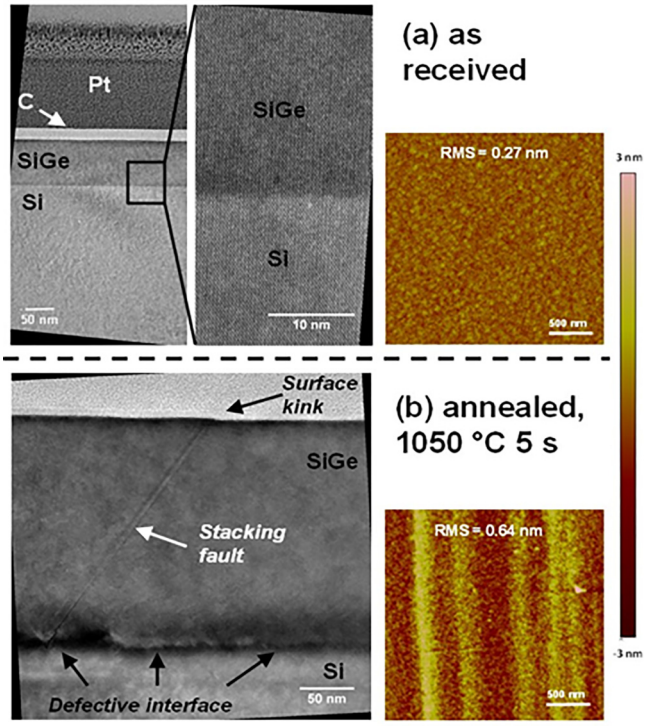


FIG. 4. XTEM and AFM of as-received SiGe 30% (top row) and SiGe 30% after annealing at 1050 °C for 5 s (bottom row).

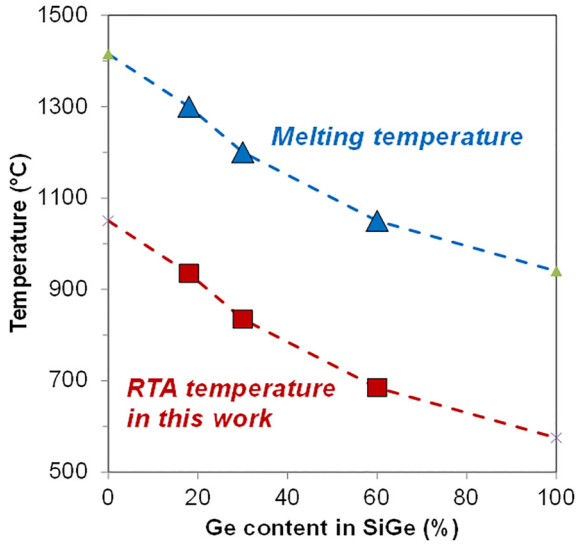


FIG. 5. Melting temperature of SiGe as a function of Ge content. The dopant drive-in RTA was chosen to be a constant value below the melting temperature, also plotted here.

Published under license by AIP Publishing.

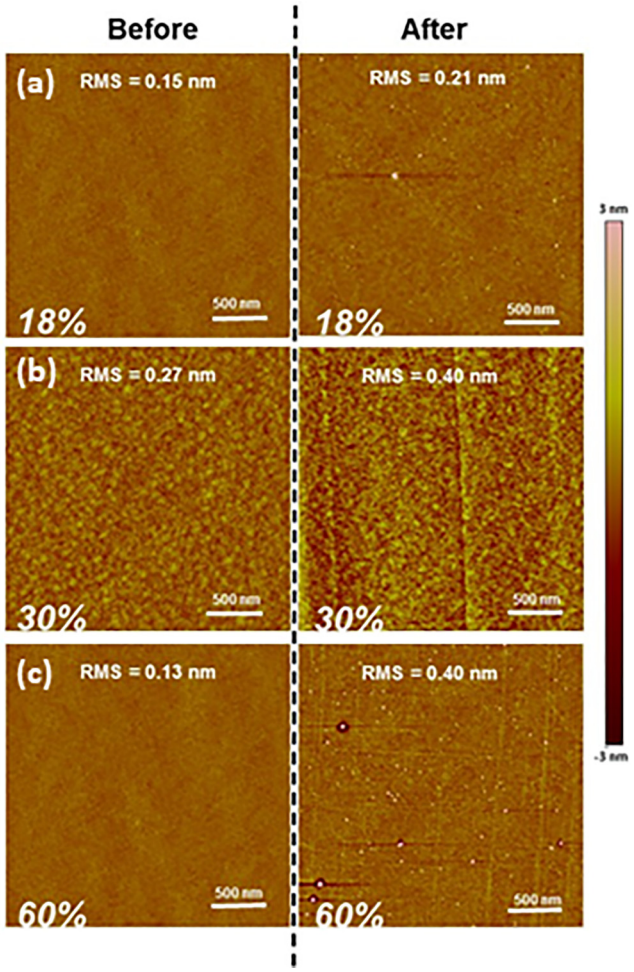


FIG. 6. AFM before (left column) and after MLD (right column) of (a) 18% SiGe, (b) 30% SiGe, and (c) 60% SiGe.

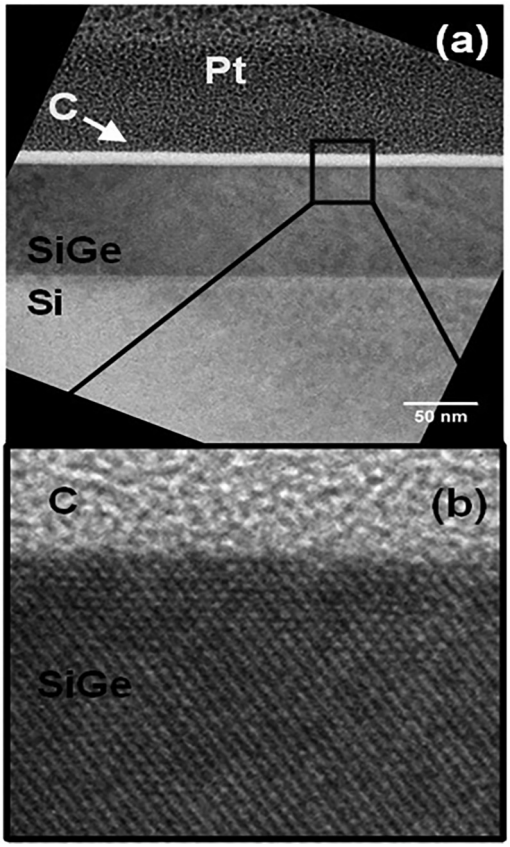


FIG. 7. (a) XTEM of SiGe30 after MLD. (b) Magnified region showing the smooth interface and crystalline SiGe.

topology is very uniform, with RMS values <0.3 nm. MLD processing leads to a small increase in all RMS values, which is to be expected with wet chemistry processing and cap addition/removal possibly leaving residue on the sample surface. Disregarding these residues due to processing, which are clearly present on the 18% and 60% after MLD, all surfaces are of good quality. Though not quantified, it is clear that crosshatching can be seen in both the 30% and 60% samples, which is an indicator of the onset of strain relaxation.[40,41]

The impact of MLD on SiGe sample quality was further probed using XTEM. Figure 7 shows images of SiGe 30% before and after MLD. It is clear from these images that P diffusion into the SiGe30 sample does not lead to any crystalline damage at the temperature used in this study. This agrees with numerous other studies that demonstrate MLD as a nondestructive doping technique.[26,42] The SiGe:Si interface in Fig. 7 does not show any evidence of defects, which leads us to believe that the small amount of crosshatching seen in AFM after MLD is inconsequential.

If defect formation as a result of strain relaxation of the SiGe layer was not considered problematic, it would be possible to utilize higher anneal temperatures up to those seen in Fig. 4 (1050 °C). These higher anneal temperatures would theoretically enable higher in-diffusion and activation of the P dopant atoms. Previous studies on silicon have found that optimal RTA temperatures for P in-diffusion and activation were somewhere in the region of 1000–1100 °C.[26,32] Another approach that may have the potential to reduce the probability of nucleating defects at the Si/SiGe interface seen at higher anneal temperatures (Fig. 4) is the use of buffer layers. These buffer layers include a gradual increase in germanium content, which leads to a smaller lattice mismatch than what is seen in samples where high-Ge content SiGe has been grown directly on Si. Alternative annealing methods such as laser annealing have also been shown to work effectively in combination with ion implantation to dope strained SiGe layers.[43] Combining laser annealing and MLD may prove to be a more suitable means than RTA, of achieving highly doped SiGe layers while maintaining the strained nature of the SiGe layer.

Published under license by AIP Publishing.

Figure 8 shows SIMS analysis of the concentration of P vs depth for the SiGe samples doped using MLD. From both Figs. 8(a) and 8(b), we note that less P diffusion occurs as the Ge content increases, again within the experimental framework of a constant $T_{melt} - T_{RTA}$, as the profiles for 18% Ge content SiGe are deeper than those in 30% Ge content SiGe, which are again deeper than those in 60% Ge content SiGe. The longer anneal time produced more diffusion, which is consistent with theory, as dopant diffusion lengths are proportional to $\sqrt{t}$, where t is the anneal time.[44] Based on the TEM images of the as-received SiGe layers, the dopant profiles in Fig. 8 are all contained within the SiGe layers, for the most part, and have not diffused into the underlying Si substrate.

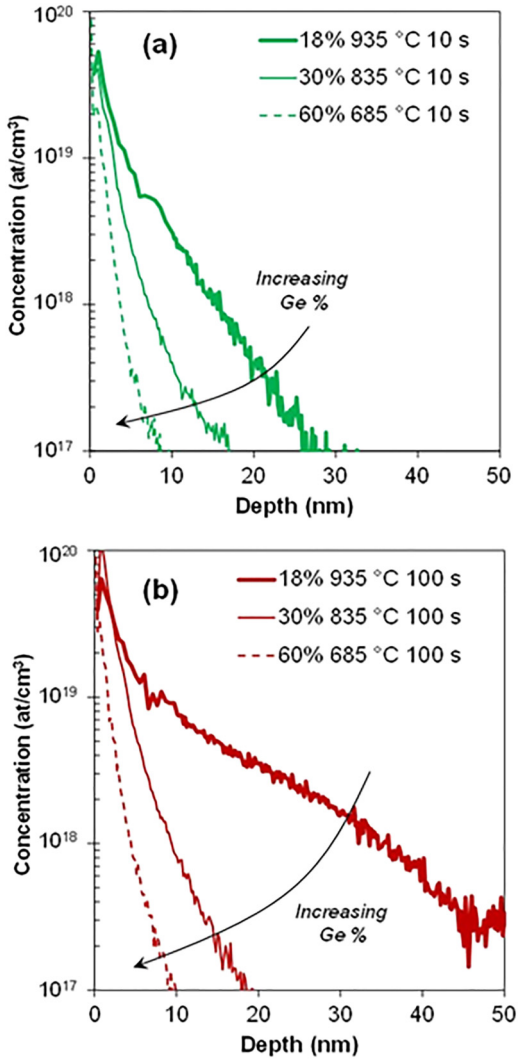


FIG. 8. SIMS of P MLD doped SiGe with concentrations of 18%, 30%, and 60% with respective annealing temperatures of 935, 835, and 685 °C at annealing times of (a) 10 s and (b) 100 s.

Figure 9 shows P-diffusivity (D) in SiGe as a function of Ge content at the specific temperatures used for the drive-in anneal. The blue points are data extracted from our experiments, while the black points are the data we could find in the literature for similar temperatures and material compositions.[45–49] The two blue points represent values extracted from the two annealing times, namely, 10 and 100 s, as shown in Fig. 8.

Note that the literature value temperatures and Ge content correspond to the experimental data we have in this work. In the literature, phosphorus D is presented as a function of 1/kT, and so for the specific content (e.g., 18% Ge), we could read off the D value for the corresponding temperature in this work (e.g., 935 °C). Overall, the values extracted from our data correspond with the trends previously reported in the literature. D drops with increasing Ge content and decreasing RTA temperature when using a constant $T_{melt} - T_{RTA}$.

The method for extracting D for in-diffused doping profiles is now briefly summarized. The impurity concentration (C) profile for a chemical predeposition process has the form

$$C_{(x,t)} = C_s erfc\left(\frac{x}{2\sqrt{Dt}}\right), \quad (1)$$

where x is the distance from the surface, t is the time, C_s is the impurity surface concentration, and D is the impurity diffusivity. If D is constant, the depth of the profile depends only on time, and the surface concentration remains fixed as this is limited by solid solubility limit at that processing temperature. If the total quantity

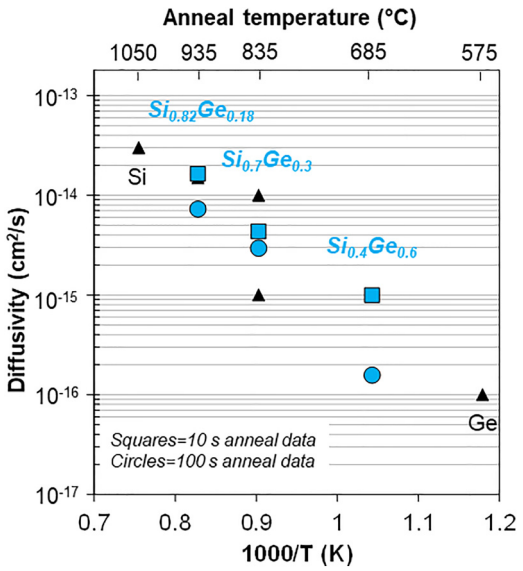


FIG. 9. Phosphorus diffusivity in SiGe vs 1000/T extracted from our experiments (blue symbols) as well as literature values (black symbols). In this case, T is the temperature of the drive-in anneal, which was kept at a constant value below the melting temperature of the material.

Published under license by AIP Publishing.

of dopant is defined as dose Q, then this can be described as

$$Q_{(t)} = \int_0^\infty C_{(x,t)}dx. \quad (2)$$

Using these two equations, the total incorporated dose can be simplified as

$$Q_{(t)} = \frac{2}{\sqrt{\pi}} C_s \sqrt{Dt}. \quad (3)$$

Using the SIMS analysis in Fig. 5, Q and C_s can be extracted. Knowing the experimental processing time, t, means D is the only unknown and thus can be calculated.

Factors that affect changes in dopant diffusivity in semiconductors include the relative dominance of interstitial-mediated or vacancy-mediated diffusion mechanisms, point-defect populations, lattice strain, presence or absence of threading dislocations and their density, and finally the dose or supply of dopant. P diffusion in Si is predominantly interstitial-mediated,[50,51] while P diffusion in Ge is vacancy-mediated.[45,52] It is not clear presently at what point along the Ge % content axis where it changes from one mechanism to the other. From the evidence in Fig. 6, diffusivity changes quite linearly rather than reaching a toggle point or falling off a cliff, so probably the switch from interstitial or vacancy mediation is gradual.

Note that this is a simplified model for the purposes of our discussion, although it is well known as a surface-source in-diffusion model. The system under study is very complicated considering that the changing alloy composition will affect diffusion mechanisms, probability of dopant-point defect pairing, intrinsic concentrations of those point defects, both charged and uncharged, as well the presence of strain and extended defects. It is not the aim of this work to go into the depth of the changing diffusion mechanisms as it would be another quite-substantial work. Furthermore, we have not explicitly considered a dependence of D on the phosphorus concentration in this surface-source in-diffusion model, mainly as concentration enhancement effects usually arise at concentrations approaching or above 10^{20} atoms/cm^3, and we are below those concentrations in this work. Nevertheless, it is important to note that we have benchmarked our results with existing reports, and the data appear consistent.

The influence of strain should also be mentioned as these SiGe layers are grown directly on a Si substrate, without a strain-relaxed-buffer (SRB). Pakfar modeled the effects of strain and Ge content on point-defect population in SiGe,[53] which drive a change in dopant diffusivity. For P, it was found that the effect of stress counterbalances the Ge chemical effect on interstitials, and thus the change in diffusivity is minimized. Note that we should state again that it was not the aim of this work to explore strain as one of the variables here, but rather to explore the choice of RTA temperature in the trade-off between successful dopant incorporation while avoiding epitaxial layer structural relaxation. Given the 2 orders of magnitude change in D as a function of RTA temperature, that is a dominant variable here.

As seen in the TEM and AFM data, with high thermal budgets, threading dislocations will form in order to relax the strained layer. The threading dislocation density (TDD) will affect the diffusivity if the material is extremely defective as these defects could form preferential pathways for P atoms to diffuse.[54] However, the data presented in Figs. 6 and 7 show that the TDD is less for the RTA temperatures considered in Figs. 8 and 9 than for the standard anneal temperature of 1050 °C. Although overall the TDD should not have a strong bearing on the conclusions in this work, we cannot conclusively state that the trend in SIMS profiles in Fig. 8 are not contributed to by the TDD.

Finally, Si and Ge interdiffusion has been modeled by Zechner and Zographos,[55] which may locally affect the SiGe composition close to the SiGe-Si interface. The change in Ge % content will have a knock-on effect on point-defect populations and hence point-defect mediated dopant diffusion, as discussed earlier. For the study here, namely, in-diffusion from the top surface, the back interface of the SiGe (away from the source of the dopant) should only have a minimal effect on the dopant drive-in.

CONCLUSIONS

This paper has outlined the application of MLD to SiGe showing both the advantages of this form of doping and some of the issues that must be overcome for future use. Ultrashallow doping has been achieved with phosphorus dopant atoms to levels currently in the region of 2×10^{19} atoms/cm^{-3}. Doping levels in excess of 1×10^{20} atoms/cm^{-3} are required for working devices, and the authors are working on combining MLD with advanced annealing processes (e.g., laser annealing) to achieve these values. Diffusivity levels found during this study agree with values from the literature for P diffusion in strained SiGe. Strain relaxation is a major issue when applying high thermal budget treatments to epitaxially grown SiGe/Si substrates. In this study, we have optimized RTA temperatures for low to high Ge content SiGe samples to produce maximum doping levels without introducing strain relaxation into the substrates. More advanced annealing methods or the use of buffer layers would allow for greater dopant incorporation while maintaining the strained nature of the SiGe layer.

ACKNOWLEDGMENTS

This work is supported by Enterprise Ireland through Project Nos. IP-2015-0368 and IP-2017-0605, and by the European Union through the European Regional Development Fund (ERDF) under Ireland's European Structural and Investment Funds Programmes 2014–2020.

REFERENCES

[1]O. Engström, B. Raeissi, S. Hall, O. Buiu, M. C. Lemme, H. D. B. Gottlob, P. K. Hurley, and K. Cherkaoui, Solid State Electron. **51**(4), 622–626 (2007).
[2]M. J. H. Van Dal, N. Collaert, G. Doornbos, G. Vellianitis, G. Curatola, B. J. Pawlak, R. Duffy, C. Jonville, B. Degroote, E. Altamirano, E. Kunnen, M. Demand, S. Beckx, T. Vandeweyer, C. Delvaux, F. Leys, A. Hikavyy, R. Rooyackers, M. Kaiser, R. G. R. Weemaes, S. Biesemans, M. Jurczak, K. Anil,

Published under license by AIP Publishing.

L. Witters, and R. J. P. Lander, in *Digest of Technical Papers—Symposium on VLSI Technology* (IEEE, 2007), pp. 110–111.
[3]J. Franco, B. Kaczer, J. Mitard, M. Toledano-Luque, G. Eneman, P. J. Roussel, M. Cho, T. Kauerauf, L. Witters, A. Hikavyy, G. Hellings, L. Å. Ragnarsson, N. Horiguchi, T. Grasser, M. Heyns, and G. Groeseneken, ECS Trans. **50**, 177–195 (2013).
[4]A. Shickova, P. Verheyen, G. Eneman, R. Degraeve, E. Simoen, P. Favia, D. O. Klenov, E. San Andres, B. Kaczer, M. Jurczak, P. Absil, H. E. Maes, and G. Groeseneken, IEEE Trans. Electron Devices **55**(12), 3432–3441 (2008).
[5]G. Eneman, S. Yamaguchi, C. Ortolland, S. Takeoka, L. Witters, T. Chiarella, P. Favia, A. Hikavyy, J. Mitard, M. Kobayashi, R. Krom, H. Bender, J. Tseng, W. E. Wang, W. Vandervorst, R. Loo, P. P. Absil, S. Biesemans, and T. Hoffmann, in *Digest of Technical Papers—Symposium on VLSI Technology* (IEEE, 2010), pp. 41–42.
[6]M. Togo, J. W. Lee, L. Pantisano, T. Chiarella, R. Ritzenthaler, R. Krom, A. Hikavyy, R. Loo, E. Rosseel, S. Brus, J. W. Maes, V. MacHkaoutsan, J. Tolle, G. Eneman, A. D. Keersgieter, G. Boccardi, G. Mannaert, S. E. Altamirano, S. Locorotondo, M. Demand, N. Horiguchi, and A. Thean, in *Technical Digest—International Electron Devices Meeting, IEDM* (IEEE, 2012), pp. 18.12.11–18.12.14.
[7]P. Hashemi, T. Ando, K. Balakrishnan, S. Koswatta, K. L. Lee, J. A. Ott, K. Chan, J. Bruley, S. U. Engelmann, V. Narayanan, E. Leobandung, and R. T. Mo, in *International Symposium on VLSI Technology, Systems and Application, VLSI-TSA 2017* (IEEE, 2017).
[8]R. Xie, P. Montanini, K. Akarvardar, N. Tripathi, B. Haran, S. Johnson, T. Hook, B. Hamieh, D. Corliss, J. Wang, X. Miao, J. Sporre, J. Fronheiser, N. Loubet, M. Sung, S. Sieg, S. Mochizuki, C. Prindle, S. Seo, A. Greene, J. Shearer, A. Labonte, S. Fan, L. Liebmann, R. Chao, A. Arceo, K. Chung, K. Cheon, P. Adusumilli, H. P. Amanapu, Z. Bi, J. Cha, H. C. Chen, R. Conti, R. Galatage, O. Gluschenkov, V. Kamineni, K. Kim, C. Lee, F. Lie, Z. Liu, S. Mehta, E. Miller, H. Niimi, C. Niu, C. Park, D. Park, M. Raymond, B. Sahu, M. Sankarapandian, S. Siddiqui, R. Southwick, L. Sun, C. Surisetty, S. Tsai, S. Whang, P. Xu, Y. Xu, C. Yeh, P. Zeitzoff, J. Zhang, J. Li, J. Demarest, J. Arnold, D. Canaperi, D. Dunn, N. Felix, D. Gupta, H. Jagannathan, S. Kanakasabapathy, W. Kleemeier, C. Labelle, M. Mottura, P. Oldiges, S. Skordas, T. Standaert, T. Yamashita, M. Colburn, M. Na, V. Paruchuri, S. Lian, R. Divakaruni, T. Gow, S. Lee, A. Knorr, H. Bu, and M. Khare, in *Technical Digest—International Electron Devices Meeting, IEDM* (IEEE, 2017), pp. 2.7.1–2.7.4.
[9]A. Ahmed, R. B. Dunford, D. J. Paul, M. Pepper, A. C. Churchill, D. J. Robbins, and A. J. Pidduck, Thin Solid Films **369**(1), 324–327 (2000).
[10]J. Zhang, S. G. Turner, S. Y. Chiam, R. Liu, E. S. Tok, A. T. S. Wee, A. C. H. Huan, I. Kelly, and C. P. A. Mulcahy, Surf. Sci. **600**(11), 2288–2292 (2006).
[11]D. Li, X. Zhao, L. Wang, B. Conrad, A. Soeriyadi, A. Lochtefeld, A. Gerger, I. Perez-Wurfl, and A. Barnett, Appl. Phys. Lett. **109**(24), 243503 (2016).
[12]L. Wang, D. Li, X. Zhao, B. Conrad, M. Diaz, A. Soeriyadi, A. Lochtefeld, A. Gerger, I. Perez-Wurfl, and A. Barnett, Phys. Status Solidi Rapid Res. Lett. **10** (8), 596–599 (2016).
[13]X. Zhao, D. Li, T. Zhang, B. Conrad, L. Wang, A. H. Soeriyadi, J. Han, M. Diaz, A. Lochtefeld, A. Gerger, I. Perez-Wurfl, and A. Barnett, Sol. Energy Mater. Sol. Cells **159**, 86–93 (2017).
[14]A. Renau, ECS Trans. **35**, 173–184 (2011).
[15]M. I. Current, *Industrial Accelerators and Their Applications* (World Scientific Publishing Co., 2012), pp. 9–56.
[16]R. Duffy, M. J. H. Van Dal, B. J. Pawlak, M. Kaiser, R. G. R. Weemaes, B. Degroote, E. Kunnen, and E. Altamirano, Appl. Phys. Lett. **90**(24), 241912 (2007).
[17]J. Mody, R. Duffy, P. Eyben, J. Goossens, A. Moussa, W. Polspoel, B. Berghmans, M. J. H. Van Dal, B. J. Pawlak, M. Kaiser, R. G. R. Weemaes, and W. Vandervorst, J. Vac. Sci. Technol. B **28**(1), C1H5–C1H13 (2010).
[18]Y. Sasaki, K. Okashita, B. Mizuo, M. Kubota, M. Ogura, and O. Nishijima, J. Appl. Phys. **111**(1), 013712 (2012).
[19]S. Sen, J. Siejka, A. Savtchouk, and J. Lagowski, Appl. Phys. Lett. **70**(17), 2253–2255 (1997).
[20]Y. Liu, K. Koga, S. Khumpuang, M. Nagao, T. Matsukawa, and S. Hara, Jpn. J. Appl. Phys. **56**(6), 06GG01 (2017).
[21]S. Shintri, C. Yong, B. Zhu, S. Byrappa, B. Fu, H. C. Lo, D. Choi, and V. Kolagunta, Mater. Sci. Semicond. Process. **82**, 9–13 (2018).
[22]J. H. Comfort, E. F. Crabbe, J. D. Cressler, W. Lee, J. Y. C. Sun, J. Malinowski, M. D'Agostino, J. N. Burghartz, J. M. C. Stork, and B. S. Meyerson, in *Technical Digest—International Electron Devices Meeting, IEDM, January 1991* (IEEE, 1991), pp. 857–860.
[23]S. Gannavaram, N. Pesovic, and M. C. Öztürk, in *Technical Digest—International Electron Devices Meeting* (IEEE, 2000), pp. 437–440.
[24]S. G. Kim, G. S. Kim, S. H. Kim, and H. Y. Yu, IEEE Electron Device Lett. **39** (12), 1828–1831 (2018).
[25]J. Veerbeek, L. Ye, W. Vijselaar, T. Kudernac, W. G. van der Wiel, and J. Huskens, Nanoscale **9**(8), 2836–2844 (2017).
[26]R. Duffy, A. Ricchio, R. Murphy, G. Maxwell, R. Murphy, G. Piaszenski, N. Petkov, A. Hydes, D. O'Connell, C. Lyons, N. Kennedy, B. Sheehan, M. Schmidt, F. Crupi, J. D. Holmes, P. K. Hurley, J. Connolly, C. Hatem, and B. Long, J. Appl. Phys. **123**(12), 125701 (2018).
[27]O. Hazut, A. Agarwala, T. Subramani, S. Waichman, and R. Yerushalmi, J. Vis. Exp. (82), e50770 (2013).
[28]J. C. Ho, R. Yerushalmi, Z. A. Jacobson, Z. Fan, R. L. Alley, and A. Javey, Nat. Mater. **7**(1), 62–67 (2008).
[29]P. Taheri, H. M. Fahad, M. Tosun, M. Hettick, D. Kiriya, K. Chen, and A. Javey, ACS Appl. Mater. Interfaces **9**(24), 20648–20655 (2017).
[30]J. C. Ho, R. Yerushalmi, G. Smith, P. Majhi, J. Bennett, J. Halim, V. N. Faifer, and A. Javey, Nano Lett. **9**(2), 725–730 (2009).
[31]T. Alphazan, L. Mathey, M. Schwarzwalder, T. H. Lin, A. J. Rossini, R. Wischert, V. Enyedi, H. Fontaine, M. Veillerot, A. Lesage, L. Emsley, L. Veyre, F. Martin, C. Thieuleux, and C. Coperet, Chem. Mater. **28**(11), 3634–3640 (2016).
[32]N. Kennedy, R. Duffy, L. Eaton, D. O'Connell, S. Monaghan, S. Garvey, J. Connolly, C. Hatem, J. D. Holmes, and B. Long, Beilstein J. Nanotechnol. **9**(1), 2106–2113 (2018).
[33]J. O'Connell, G. Collins, G. P. McGlacken, R. Duffy, and J. D. Holmes, ACS Appl. Mater. Interfaces **8**(6), 4101–4108 (2016).
[34]M. van Druenen, G. Collins, C. Glynn, C. O'Dwyer, and J. D. Holmes, ACS Appl. Mater. Interfaces **10**(2), 2191–2201 (2018).
[35]B. Long, G. A. Verni, J. O'Connell, J. Holmes, M. Shayesteh, D. O'Connell, R. Duffy, and IEEE, in *2014 20th International Conference on Ion Implantation Technology (IIT 2014)* (IEEE, 2014), p. 4.
[36]B. Long, G. A. Verni, J. O'Connell, M. Shayesteh, A. Gangnaik, Y. M. Georgiev, P. Carolan, D. O'Connell, K. J. Kuhn, S. B. Clendenning, R. Nagle, R. Duffy, and J. D. Holmes, Mater. Sci. Semicond. Process. **62**, 196–200 (2017).
[37]F. Sgarbossa, S. M. Carturan, D. De Salvador, G. A. Rizzi, E. Napolitani, G. Maggioni, W. Raniero, D. R. Napoli, G. Granozzi, and A. Carnera, Nanotechnology **29**(46), 465702 (2018).
[38]J. O'Connell, E. Napolitani, G. Impellizzeri, C. Glynn, G. P. McGlacken, C. O'Dwyer, R. Duffy, and J. D. Holmes, ACS Omega **2**(5), 1750–1759 (2017).
[39]S. Tanuma, C. J. Powell, and D. R. Penn, Surf. Interface Anal. **43**(3), 689–713 (2011).
[40]H. Chen, Y. K. Li, C. S. Peng, H. F. Liu, Y. L. Liu, Q. Huang, J. M. Zhou, and Q. K. Xue, Phys. Rev. B **65**(23), 4 (2002).
[41]T. Egawa, A. Sakai, T. Yamamoto, N. Taoka, O. Nakatsuka, S. Zaima, and Y. Yasuda, Appl. Surf. Sci. **224**(1–4), 104–107 (2004).
[42]J. O'Connell, S. Biswas, R. Duffy, and J. D. Holmes, Nanotechnology **27**, 342002 (2016).
[43]G. V. Luong, S. Wirths, S. Stefanov, B. Holländer, J. Schubert, J. C. Conde, T. Stoica, U. Breuer, S. Chiussi, M. Goryll, D. Buca, and S. Mantl, J. Appl. Phys. **113**(20), 204902 (2013).
[44]P. M. Fahey, P. B. Griffin, and J. D. Plummer, Rev. Mod. Phys. **61**(2), 289–384 (1989).
[45]S. Brotzmann and H. Bracht, J. Appl. Phys. **103**(3), 033508 (2008).

Published under license by AIP Publishing.

[46]J. S. Christensen, H. H. Radamson, A. Y. Kuznetsov, and B. G. Svensson, J. Appl. Phys. **94**(10), 6533–6540 (2003).
[47]N. R. Zangenberg, J. Fage-Pedersen, J. L. Hansen, and A. N. Larsen, J. Appl. Phys. **94**(6), 3883–3890 (2003).
[48]D. Mathiot and J. C. Dupuy, Appl. Phys. Lett. **59**(1), 93–95 (1991).
[49]P. Pichler, *Intrinsic Point Defects, Impurities, and Their Diffusion in Silicon* (Springer, Wien, 2004).
[50]J. Xu, V. Krishnamoorthy, K. S. Jones, and M. E. Law, J. Appl. Phys. **81**(1), 107–111 (1997).
[51]N. E. B. Cowern, D. J. Godfrey, and D. E. Sykes, Appl. Phys. Lett. **49**(25), 1711–1713 (1986).
[52]M. Naganawa, Y. Shimizu, M. Uematsu, K. M. Itoh, K. Sawano, Y. Shiraki, and E. E. Haller, Appl. Phys. Lett. **93**(19), 191905 (2008).
[53]A. Pakfar, Mater. Sci. Eng. B **89**(1–3), 225–228 (2002).
[54]N. Kuroda, C. Sasaoka, A. Kimura, A. Usui, and Y. Mochizuki, J. Cryst. Growth **189–190**, 551–555 (1998).
[55]C. Zechner and N. Zographos, Mater. Sci. Semicond. Process. **42**, 230–234 (2016).

Published under license by AIP Publishing.